BIODIVERSITAS
Volume 26, Number 7, July 2025
Pages: 3469-3483

ISSN: 1412-033X
E-ISSN: 2085-4722
DOI: 10.13057/biodiv/d260737

GC-MS profiling and molecular docking of bioactive compounds from *Strychnos lucida* on reproductive protein targets

ST. AISYAH SIJID[1,3,♥], HERRY SONJAYA[2], RATMAWATI MALAKA[2], HASBI HASBI[2,♥♥]

[1]Doctoral Program, Department of Animal Science, Faculty of Animal Science, Universitas Hasanuddin. Jl. Perintis Kemerdekaan Km. 10, Makassar 90245, South Sulawesi, Indonesia. Tel./fax.: +62-411-585466, ♥email: aisyahsijid@gmail.com

[2]Department of Animal Production, Faculty of Animal Science, Universitas Hasanuddin. Jl. Perintis Kemerdekaan Km. 10, Makassar 90245, South Sulawesi, Indonesia. Tel./fax.: +62-411-585466, ♥email: hasbi_fapetunhas@yahoo.com

[3]Department of Biology, UIN Alauddin Makassar. Jl. H.M. Yasin Limpo No. 36, Gowa 92118, South Sulawesi, Indonesia

Manuscript received: 21 February 2025. Revision accepted: 25 July 2025.

Abstract. *Sijid SA, Sonjaya H, Malaka R, Hasbi H. 2025. GC-MS profiling and molecular docking of bioactive compounds from* Strychnos lucida *on reproductive protein targets. Biodiversitas 26: 3469-3483. Strychnos lucida*, locally known as *Kayu Ular* (KU), is traditionally used in various regions of Indonesia, commonly used to enhance stamina and vitality, with anecdotal claims suggesting benefits related to reproductive function. This study aimed to evaluate the plant's potential in reproductive health through phytochemical screening, Fourier Transform Infrared Spectroscopy (FTIR), Gas Chromatography-Mass Spectrometry (GC-MS), and molecular docking analysis. The extract was obtained by macerating the plant material in 96% ethanol. Phytochemical screening confirmed the presence of flavonoids, alkaloids, tannins, and saponins, which are associated with antioxidant, anti-inflammatory, and hormonal modulatory activities. Among them, flavonoids and saponins are particularly known to improve fertility enhancement and hormonal balance. A total of 66 compounds were identified by GC-MS, with Lunacrine (52.71%) as the most abundant. Molecular docking was conducted on four dominant compounds—Lunacrine, (Z)-11-octadecenoic acid, hexadecanoic acid, and (9Z,12Z)-octadeca-9,12-dienoic acid—against five reproductive-related protein targets: AMPK, SIRT1, COX-2, PPAR-α, and Dynein. Lunacrine exhibited strong binding affinities with the target receptors AMPK (-7.8 kcal/mol), SIRT1 (-8.5 kcal/mol), and COX-2 (-8.9 kcal/mol), suggesting its potential to modulate energy metabolism, oxidative stress, and inflammation—critical processes in hormonal regulation and reproductive function. These findings support the traditional use of *S. lucida* for reproductive health and highlight Lunacrine as a promising candidate for further phytopharmaceutical development. Follow-up in vitro and in vivo studies are recommended to validate its therapeutic potential.

Keywords: Alkaloid compound, binding affinity, FTIR, GC-MS, Lunacrine

INTRODUCTION

Reproductive health is a cornerstone of individual and societal well-being, encompassing the physical, mental, and social dimensions of the reproductive system and its functions (WHO 2018; Starrs et al. 2018). The ability to maintain healthy reproductive lives underpins social and economic progress and involves preventing endocrine disorders, managing sexually transmitted infections, and safeguarding reproductive rights (Engel et al. 2019; Fumagalli et al. 2024; Sladden et al. 2021). In this context, interest in culturally accepted, affordable interventions—especially medicinal plants—has intensified.

Among these, *Strychnos lucida* R.Br. (locally known as *Kayu Ular*, KU), a member of the pantropical genus *Strychnos* (Loganiaceae), has attracted increasing attention. The genus includes ~200 species distributed across tropical regions, many with documented pharmacological activities in Indonesia. *S. lucida*—also referred to as *S. ligustrina*—is widely distributed in West and East Nusa Tenggara, Sulawesi, Kalimantan, Java, and Papua and is known by vernacular names such as *bidara laut*, *dara putih*, and *kayu ular* (Laumonier and Nasi; 2018; Setyayudi et al. 2019; Gunawan et al. 2022). Ethnomedicinal reports describe *S. lucida* as a remedy for vitality and reproductive health, yet evidence-based options remain scarce. Preliminary findings support its traditional use: decoctions of *S. lucida* reduced sperm abnormalities in diabetic mouse models (Kunu et al. 2020). However, this remains the only documented in vivo reproductive study, underscoring the need for mechanistic exploration.

Phytochemical analyses have revealed diverse metabolites in *S. lucida*, including alkaloids, flavonoids, tannins, and saponins (Manurung et al. 2019; Travasarou et al. 2019; Makani et al. 2025). These compound classes are linked to biological activities relevant to reproductive health: flavonoids enhance ovarian function via estrogen receptor modulation and antioxidant effects (Adewoyin et al. 2017); saponins stimulate luteinizing hormone secretion to support ovulation (Cui et al. 2023); and alkaloids contribute to anti-inflammatory and energy-regulatory pathways (Li et al. 2020; Patalas-Krawczyk et al. 2021; Khasanah et al. 2022). While these findings establish a biochemical rationale for traditional use, the molecular pathways through which *S. lucida* affects reproductive physiology remain unclear.

Computational tools, particularly molecular docking, offer an efficient starting point to address this gap. Docking predicts ligand-protein interactions and estimates binding

energies, enabling prioritization of bioactive compounds for further study (Bhati et al. 2017; Surpeta et al. 2020; Chang et al. 2022). It also identifies hydrogen bonds, hydrophobic contacts, and residue-level interactions, while root mean square deviation (RMSD) assesses docking accuracy (Cournia et al. 2017; Kulandaisamy et al. 2017; Pagadala et al. 2017). Such methods accelerate early drug discovery and help narrow candidates for in vitro and in vivo validation (Agamah et al. 2020; Singh and Pathak, 2020; Wan et al. 2020; Younus et al. 2021).

To investigate *S. lucida*'s pharmacological potential, this study integrates phytochemical screening, Fourier Transform Infrared Spectroscopy (FTIR), and Gas Chromatography-Mass Spectrometry (GC-MS) to profile metabolites, followed by docking simulations against key reproductive protein targets. The selected targets—AMP-activated protein kinase (AMPK), sirtuin 1 (SIRT1), cyclooxygenase-2 (COX-2), peroxisome proliferator-activated receptor alpha (PPAR-α), and dynein. AMPK serves as an energy sensor essential for gamete quality and metabolism (Martin-Hidalgo et al. 2018); SIRT1 modulates oxidative stress and deacetylation pathways (Liu et al. 2018; Zhao et al. 2020); COX-2 governs prostaglandin synthesis required for ovulation (Sugimoto et al. 2015); PPAR-α regulates lipid metabolism and hormonal balance (Bougarne et al. 2018; Przybycień et al. 2022); and dynein is crucial for intracellular transport and gamete maturation (Inaba and Mizuno 2016; Canty et al. 2021).

By linking ethnomedicinal knowledge with chemical profiling and computational docking, this study provides the first integrated assessment of *S. lucida* bioactive compounds on reproductive protein targets. This combined FTIR/GC-MS and docking approach establishes a scientific foundation for prioritizing compounds for future pharmacological, pharmacokinetic, and toxicological evaluation, bridging traditional knowledge and modern reproductive pharmacology.

MATERIALS AND METHODS

Ethanol extraction of *Strychnos lucida*

Strychnos lucida (KU) were collected from Kaluppini Village, Enrekang District, South Sulawesi, Indonesia. KU plant was cleaned with running water, sliced thinly, and dried at 50°C using an oven, and was then ground using a blender until it formed a fine powder, which was sifted to obtain a finer particle size (Krakowska-Sieprawska et al. 2022). The KU powder was macerated with 96% ethanol as a solvent for 72 hours, and the filtrate was evaporated using a rotary evaporator to obtain a concentrated extract (Fonmboh et al. 2020).

The use of 96% ethanol was based on its efficiency in extracting a broad spectrum of phytochemicals, particularly semi-polar to non-polar compounds such as alkaloids, flavonoids, and saponins, which are commonly present in medicinal plants like *S. lucida* (Azwanida 2015). Additionally, preliminary observations and literature indicated that high-concentration ethanol enhances compound solubility and prevents microbial growth during maceration. This solvent was selected to maximize extraction yield and preserve bioactive constituents.

Phytochemical screening

Phytochemical screening of the KU extract was conducted to detect the presence of flavonoids, alkaloids, terpenoids, steroids, tannins, and saponins, following the method of Dubale et al. with modifications. Flavonoids were tested by mixing 2 mL of extract with 1 mL of 2 N sodium hydroxide (NaOH), resulting in a yellow color indicating the presence of flavonoids. Alkaloids were tested by mixing 2 mL of hydrochloric acid with 2 mL of extract, followed by adding a few drops of Meyer's reagent, which produced a green color or white precipitate as evidence of alkaloids. Furthermore, terpenoids were tested by adding 2 mL of chloroform and sulfuric acid to extract; the presence of a reddish-brown color at the interface indicated the presence of terpenoids. Steroids were detected by mixing the extract with chloroform and sulfuric acid, producing a copper-brown ring at the interface as an indication of steroids. Tannins were tested by mixing the extract with a 5% $FeCl_3$ solution, which resulted in a dark blue or greenish-black color as a sign of tannins. Finally, saponins were tested by mixing extracts with distilled water and shaking for 15 minutes, which resulted in a foam layer of 1 cm height as an indication of saponins (Dubale et al. 2023).

Functional group identification via FTIR

1.5-2.0 g of the extract was slowly mixed with 200 mg of solid KBr and ground to form pellets. Standard equipment was used to prepare the pellets under vacuum and pressure (75 kN cm^{-2}) for 2-3 minutes. These pellets were then used for functional group spectral analysis using FTIR (Thermo Fisher Scientific, USA), and the spectral resolution was 4 cm^{-1} with a scanning range of 400-4000 cm^{-1} (Özgenç et al. 2017).

Identification of compounds using GC-MS

Secondary metabolites were identified using Gas Chromatography-Mass Spectrometry (GC-MS), aiming to profile bioactive compounds and assess the presence of potentially toxic constituents, considering the known toxicity of particular Strychnos species. The test sample was mixed with 5 mL of 96% ethanol (p.a.). Extraction was carried out using ultrasonic treatment for 30 minutes at 55°C. The mixture was then filtered using Whatman No. 42 filter paper and injected into the GC-MS. This instrument conditions (Shimadzu Ultra QP 2010) were set as follows: injector temperature at 250°C in Splitless mode, pressure at 76.9 kPa, flow rate of 14 mL/min, and a split ratio of 1:10. The ion source and interface temperatures were set to 200°C and 280°C, respectively, with a solvent cut time of 3 minutes, and the mass range scanned was from 400 to 700 m/z. The column used was SH-Rxi-5Sil MS, with a column length of 30 m and an inner diameter of 0.25 mm. The initial column temperature was set to 70°C with a hold time of 2 minutes, then increased to 200°C at a rate of 100°C/min, and the final temperature was increased to 280°C with a hold time of 9 minutes at a rate of 50°C/min, giving a total analysis time of 36 minutes. The chromatogram

data obtained were analyzed using the NIST 17 and Wiley 9 libraries (Tsugawa and Fukusaki 2020).

Molecular docking

Protein and ligand preparation

Protein structures were retrieved from the Protein Data Bank (http://www.rcsb.org/pdb/) and processed using PyMOL 2.5.4 by removing crystallographic water molecules, co-crystallized ligands, and non-standard residues (Sembiring et al. 2023; Kumar et al. 2024). Five targets with established roles in reproductive function were selected: AMPK (PDB ID: 4CFF), SIRT1 (4ZZI), COX-2 (6COX), PPAR-α (3VI8), and Dynein (8I3J). These proteins regulate energy metabolism, oxidative stress response, inflammation, hormonal balance, and intracellular transport—processes critically involved in fertility and reproductive health (Inaba and Mizuno 2016; Bougarne et al. 2018; Martin-Hidalgo et al. 2018). Ligand structures were obtained from the PubChem database, energy-minimized using Open Babel, and converted to PDBQT format via PyRx 0.8 (Tuli et al. 2022).

Docking setup

Molecular docking was conducted using AutoDock Vina within the PyRx 0.8 interface, with the exhaustiveness set to 8. Grid boxes were generated to fully encompass the predicted binding pockets of each protein. The top-ranked docking pose (lowest ΔG) for each ligand-protein complex was selected for further analysis. SwissADME (http://www.swissadme.ch) was used to assess pharmacokinetic parameters, including Lipinski's Rule of Five compliance (Yueniwati et al. 2021).

Docking validation

Protocol validation was attempted by redocking the co-crystallized ligand SC-558 into COX-2 (PDB ID: 6COX). The crystallographic pose was used as a reference (RMSD = 0.0 Å). Redocking produced poses with competitive binding affinities (-7.8 to -8.9 kcal/mol) but high RMSD values (14-34 Å), indicating a notable deviation from the native ligand pose. The high RMSD values likely reflect the use of a large, fully encompassing grid box and rigid docking parameters, which may have allowed SC-558 to adopt alternative low-energy poses outside its crystallographic binding orientation. SC-558 binds at a relatively specific COX-2 allosteric site, and without residue flexibility or grid refinement, redocked poses can diverge substantially from the native pose despite retaining favorable binding energies. Considering the exploratory scope of this study, further refinement (e.g., grid adjustment or flexible docking) was not performed; instead, the same standardized docking parameters were uniformly applied across all protein targets to maintain methodological consistency. For targets lacking co-crystallized ligands or PubChem references, RMSD-based validation could not be performed.

Visualization

Ligand-protein complexes were examined using Discovery Studio Visualizer 2024 Client (version 24.1) to identify hydrogen bonds, hydrophobic contacts, and π-alkyl interactions, confirming that the predicted docking poses remained chemically plausible despite RMSD limitations.

RESULTS AND DISCUSSION

Phytochemical screening

Phytochemical screening on the KU extract showed positive results for flavonoids, alkaloids, tannins, and saponins, as shown in Table 1. Terpenoids and steroids showed negative results.

FTIR and GC-MS identification

FTIR analysis of the *Strychnos lucida* extract (KU) in the range of 4000-400 cm^{-1} revealed the presence of various functional groups consistent with phytochemically active constituents (Figure 1). The broad absorption band at 3398.04 cm^{-1} corresponds to O-H stretching vibrations, typically associated with hydroxyl groups in alcohols or phenolic compounds (Pasieczna-Patkowska et al. 2025). The broadening of this peak may indicate the formation of hydrogen bonding, which is common in complex plant extracts. The C-H stretching vibrations at 2926.15 cm^{-1} and 2855.72 cm^{-1} suggest the presence of aliphatic chains, such as $-CH_2-$ and $-CH_3$ groups, characteristic of saturated hydrocarbons (Smith 2022).

A sharp peak at 1700.21 cm^{-1} indicates C=O stretching, suggesting the presence of carbonyl-containing compounds such as ketones, aldehydes, or carboxylic acids. Peaks at 1605.18 cm^{-1}, 1634.50 cm^{-1}, and 1462.56 cm^{-1} likely correspond to aromatic C=C stretching vibrations, indicating aromatic rings or conjugated systems. The fingerprint region (1500-500 cm^{-1}) displays multiple, somewhat overlapping peaks—including those at 1365.97, 1286.08, 1204.54, 1074.22, and 1034.50 cm^{-1}—which may represent C-H bending, C-O stretching (alcohols, ethers, or esters), and possibly C-N vibrations. The complex overlapping and broadening in this region reflect the diverse nature of phytochemicals and may pose limitations in peak specificity without further spectroscopic support (Nandiyanto et al. 2023).

Table 1. Phytochemical analysis of KU extract revealed the presence of various compounds, as indicated by the (+) symbol

Class of compound (test type)	Color change	Test result
Flavonoid		
Conc.H_2SO_4	Dark yellow solution	+
NaOH 10%	Dark yellow solution	+
$FeCl_3$ 5%	Yellow-green solution	+
Alkaloid		
Meyer	Yellow solution (with white precipitate)	+
Dragendorff	Brown precipitate formed	+
Wagner	Orange precipitate formed	+
Terpenoid and steroid	Yellow solution	-
Tanin	Light yellow solution	+
Saponin	Foam formation	+

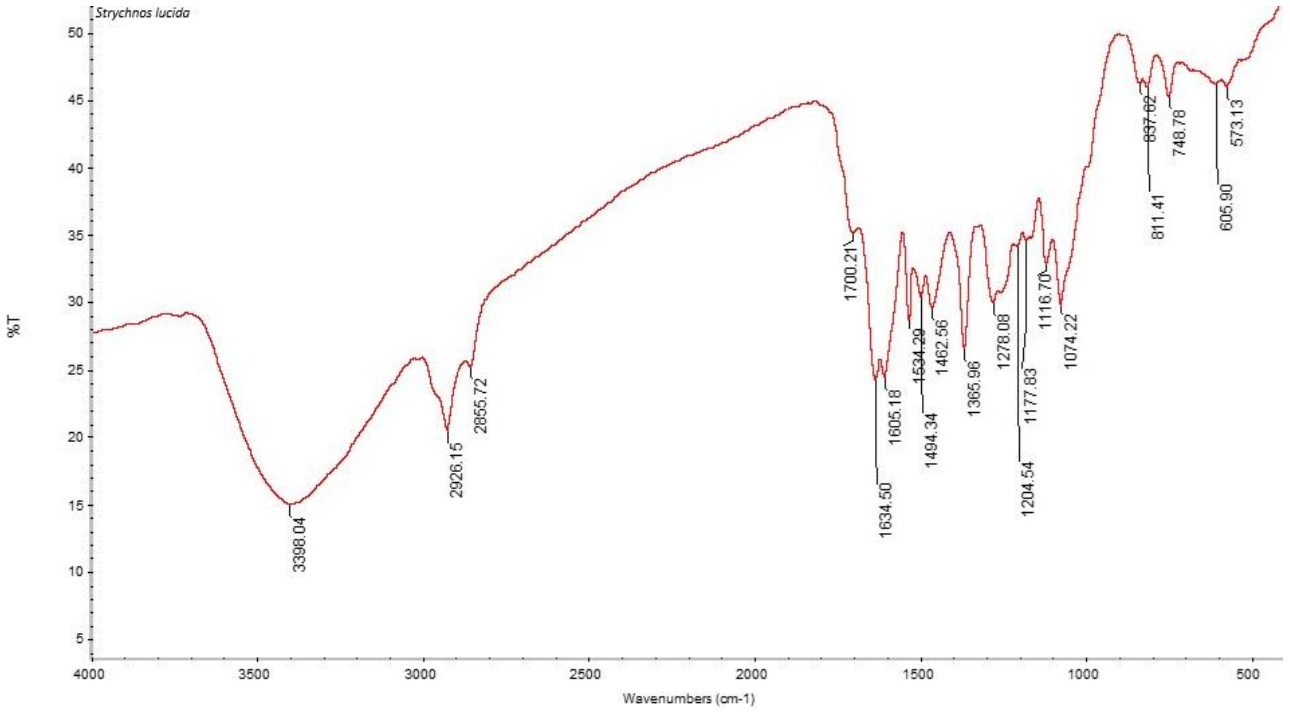

Figure 1. FTIR spectrum of KU extract in the 4000-400 cm^{-1} range

GC-MS analysis of the KU extract revealed a chemically diverse profile, as shown in the total ion chromatogram (Figure 2 and Table 2), which displayed 66 identified peaks. Compound identification was performed through spectral matching with the NIST 17 and Wiley 9 libraries, successfully annotating all 66 peaks. This relatively high number aligns with the documented phytochemical richness of the *Strychnos* genus (Rahayu et al. 2022; Alagbe 2023; Cassas et al. 2025). It highlights the efficiency of ethanol as a polar solvent capable of extracting a wide range of metabolite classes (Ibrahim et al. 2021).

The number of peaks detected is consistent with expectations based on the genus' known metabolic diversity, and no substantial deviation (such as peak scarcity or overload) was observed. Notably, Lunacrine (52.71%) and Balfourodine (15.67%) emerged as the most dominant constituents, accounting for more than 68% of the total chromatographic area. This level of dominance is higher than typically reported in other *Strychnos* species, where no single compound usually exceeds 20% relative abundance, suggesting possible chemotypic variation or extraction-specific enrichment. Meanwhile, the absence of alkaloids such as strychnine or brucine—frequently observed in other *Strychnos* species—may be attributed to differences in ecological factors or solvent selectivity. The percentages presented in the GC-MS table represent the relative abundance of each compound, calculated from the total integrated area of all detected peaks in the chromatogram. Thus, the values reflect the proportion of each compound relative to the entire volatile profile of the extract, as determined by the GC-MS analysis. Among these, ten compounds were identified as dominant based on their relative peak areas: Lunacrine (52.71%), Balfourodine (15.67%), Benzo[octahydroacephenanthrylene] (7.48%), 1,3,4,5-Tetrahydroxycyclohexanecarboxylic acid (2.50%), Isobalfourodine (0.96%), (Z)-11-Octadecenoic acid (0.90%), Hexadecanoic acid (0.42%), (9Z,12Z)-Octadeca-9,12-dienoic acid (0.10%), Methyl 4-hydroxy-3-methoxybenzoate (0.02%), and Neophytadiene (0.01%).

Molecular docking

Molecular docking analysis was performed to evaluate the interaction potential of KU compounds in improving reproductive health. Based on the confirmation from GC-MS and FTIR, four compounds most relevant to reproductive health were selected, and the pharmacokinetic profiles of the selected compounds are shown in Table 3.

The pharmacokinetic parameters included molecular weight, hydrogen bond donors and acceptors, lipophilicity (cLogP), and Topological Polar Surface Area (TPSA), as predicted using the SwissADME tool (Daina et al. 2017). These parameters were selected to assess basic drug-likeness and absorption potential; however, it is important to note that this is not a comprehensive pharmacokinetic profile, as it does not include critical in vivo properties such as bioavailability, metabolic half-life, or clearance.

Molecular docking between the ligand and target protein was performed using the Vina Wizard in the PyRx program. The optimum conformation between the protein and ligand from molecular docking results could be selected from the ligand conformation with the highest binding affinity (lowest value). The binding affinity of the ligand and target protein interaction is presented in Table 4.

Table 2. Identified compounds in the KU extract using GC-MS analysis

Compound	Peak area	Retention-time	A/H ratio	Total area percentage	Index similarity	Molecular weight (g/mol)	Chemical class
2-Ethylhexanal	303954	3.496	3.17	0.01	91	128	Aliphatic aldehyde
3-Methyl-1-butanol	1336232	3.836	4.01	0.05	98	88	Aliphatic alcohol
3,3-Dimethoxy-2-butanone	194434	5.060	2.45	0.01	84	132	Ketone
2-Ethyl-1,3-dioxolane-4-methanol	109782	5.159	2.21	0.00	79	132	Cyclic alcohol and ether
trans-Shisool	347448	13.931	5.38	0.01	77	154	Terpenoid alcohol
(1R,7R,7aS)-1,7-Dimethyl-7-(4-methylpent-3-enyl)bicyclo[2.2.1]heptane	194987	14.325	3.02	0.01	91	204	Terpenoid
(5Z,8Z,11Z)-Eicosatrienoic acid	44151	14.400	2.02	0.00	53	378	Unsaturated fatty acid (PUFA)
2,6-Dimethyl-6-(4-methylpent-3-enyl)bicyclo[3.1.1]hept-2-ene	241784	14.513	3.69	0.01	91	204	Terpenoid
(1S,6Z,8S,9Z)-8-Isopropyl-1-methyl-5-methylenecyclodeca-1,6-diene	286628	15.236	2.87	0.01	89	204	Cyclic terpenoid
(E)-β-Bisabolene	786592	15.528	3.47	0.03	95	204	Aromatic alcohol
1-(1-Methylethyl)-4,7-dimethyloctahydronaphthalene	87387	15.683	2.60	0.00	78	204	Sesquiterpene hydrocarbon
Methyl 4-hydroxy-3-methoxybenzoate	605068	16.142	7.39	0.02	77	182	Aliphatic alcohol
1,6-Anhydro-β-D-glucopyranose	1190248	16.325	10.47	0.05	89	162	Terpenoid alcohol
4-Ethenyl-2,6-dimethoxyphenol	2306813	16.558	7.23	0.09	80	180	Aromatic ester (UV filter)
1,5,9-Trimethyl-12-(1-methylethyl)-4,8,13-cyclotetradecatriene-1,3-diol	393136	16.675	2.64	0.01	58	306	Saturated alkane (hydrocarbon)
1,1,4,7-Tetramethyldecahydro-1H-cyclopropa[e]azulen-4-ol	933294	16.780	4.34	0.04	95	222	Sesquiterpene alcohol
4-Hydroxy-3-methoxybenzoic acid	457840	17.258	6.24	0.02	74	168	Phenolic acid (vanillic derivative)
α-Cadinol	452999	17.363	4.09	0.02	85	222	Sesquiterpene alcohol
(1R,3R,4R,5R)-Quinic acid	3610812	17.671	9.91	0.14	74	192	Polycarboxylic acid (polyol carboxylic acid)
1,3,4,5-Tetrahydroxycyclohexanecarboxylic acid	66034167	18.212	21.52	2.50	95	192	Polyol acid
Methyl 1-methyl-2-oxocyclohexanecarboxylate	437042	18.875	5.46	0.02	68	170	Cyclic ester
4-Hydroxy-3,5-dimethoxybenzoic acid hydrazide	3228446	19.001	7.39	0.12	96	212	Phenolic hydrazide
Neophytadiene	197231	19.575	2.48	0.01	93	278	Diterpenoid hydrocarbon
3-Hydroxy-4,5-dimethoxybenzoic acid	2262084	20.258	11.43	0.09	83	198	Phenolic acid
1-(α-Ethenyldecahydro-2-hydroxy)naphthalenepropanol	293626	20.517	4.45	0.01	63	308	Cyclic aromatic alcohol
Methyl hexadecanoate	1610016	21.080	3.28	0.06	97	270	Fatty acid ester (methyl palmitate)
Methyl 3,5-bis(1,1-dimethylethyl)-4-hydroxybenzoate	1139546	21.253	3.32	0.04	91	292	Phenolic ester
Hexadecanoic acid	11130056	22.043	5.41	0.42	96	256	Saturated fatty acid (SFA)
Ethyl hexadecanoate	267978	22.476	3.36	0.01	91	284	Fatty acid ester (ethyl palmitate)
Methyl (9Z,12Z)-octadeca-9,12-dienoate	2679693	24.899	3.68	0.10	96	294	PUFA ester (methyl linoleate)
Methyl (Z)-octadec-6-enoate	7343900	25.055	3.72	0.28	90	296	MUFA ester (methyl oleate)
Methyl octadecanoate	310320	25.668	3.44	0.01	95	298	Saturated fatty acid ester
(9Z,12Z)-Octadeca-9,12-dienoic acid	5559892	26.098	5.59	0.21	96	280	PUFA (omega-6)
(Z)-11-Octadecenoic acid	23795638	26.260	6.58	0.90	90	282	MUFA
Ethyl linoleate	2446558	26.425	5.78	0.09	86	308	PUFA ester
Ethyl oleate	2315536	26.572	5.18	0.09	89	310	MUFA ester
Octadecanoic acid	1261970	26.735	6.52	0.05	91	284	Saturated fatty acid (stearic acid)

2,2,6-Trimethyl-2H,SH-pyrano[3,2-c]quinolin-5-one	1413168	26.890	8.05	0.05	90	241	Alkaloid / quinolone derivative
1-(3-Methylphenyl)cyclohexyl)piperidine	1534859	28.515	5.61	0.06	64	257	Aromatic piperidine (synthetic alkaloid?)
2-Methyl-3-heptyl-4-(ethoxycarbonyloxy)-7-methoxyquinolone	1067089	29.989	5.40	0.04	67	259	Quinolone ester
N,N-Bis(trifluoromethyl)-2,6-diethylaniline	380955	30.740	4.06	0.01	55	341	Aniline derivative
4,7,8-Trimethoxyfuro[2,3-b]quinoline	1393281	31.134	6.57	0.05	94	259	Methoxylated quinoline
4-Ethyl-9-phenylbenz[f]indole	8305203	31.381	6.55	0.32	64	271	Polycyclic indole
Platydesmine	5781702	31.720	7.15	0.22	72	259	Methoxy indole alkaloid
5-[1-(3,3-Dimethyl-5-oxopyrrolidin-2-ylidene)-2-oxoethyl]-2,3,3-trimethyl-2,3-dihydro-1	83147412	32.588	5.03	3.15	66	287	Indole-pyrrolidone complex
4-(3,4-Dimethoxyphenyl)-1-methyl-4H-pyrazolo[3,4-b]pyridin-6-one	7834050	32.852	6.19	0.30	58	287	Aromatic heterocycle (pyrazole derivative)
Lunacrine	10258645	32.941	5.50	0.39	79	273	Alkaloid (indole acridone)
N-Phenyl-N-(3,4-dimethoxybenzylidene)hydrazine	4837116	33.106	6.36	0.18	63	256	Aromatic hydrazone
6,7-Methylenedioxy-9-acetylcarbazole	20426405	33.286	5.94	0.77	66	273	Carbazole alkaloid
Lunacrine	33094569	33.568	11.37	1.26	82	273	Alkaloid (identical to compound 47)
Benzo[octahydroacephenanthrylene]	197249745	33.939	7.89	7.48	64	260	Tricyclic aromatic compound
2,2-Bis(1H-indol-2-yl)propanenitrile	4179120	34.300	11.04	0.16	62	285	Indole alkaloid dimer
4,5-Dihydro-8-methoxy-2-methylnaphtho[1,2-d]thiazole	4766696	34.567	8.23	0.18	76	231	Aromatic thiazole derivative
4-Chlorophenyl 4-(methoxymethyl)-6-methyl-3-(1H-pyrrol-1-yl)	2104188	34.823	7.47	0.08	60	412	Chlorinated heterocycle
3-Isopentenyl-4,7,8-trimethoxyquinolin-2-one	14112498	35.188	5.48	0.54	61	303	Methoxylated furoquinoline
(E)-2-[2-(3,4-Dimethoxyphenyl)ethenyl]pyrrolidine	136699680	35.410	6.27	5.18	57	233	Stilbene-alkaloid derivative
Lunacrine	8760748	35.661	9.15	0.33	72	273	Alkaloid
Balfourodine	413168153	36.250	15.89	15.67	66	289	Alkaloid
Isobalfourodine	25219701	36.461	8.48	0.96	77	289	Alkaloid
Lunacrine	1389821910	37.340	29.58	52.71	94	273	Alkaloid
Arctinone A	861513	37.800	8.58	0.03	62	262	Lignan (complex phenolic)
5-(4-Tert-butylphenyl)-4-methyl-4H-[1,2,4]triazole-3-thiol	43698137	38.154	6.23	1.66	70	247	Aromatic triazole
7,8-Dihydro-8-(2-hydroxypropan-2-yl)-1,3-dioxolo[4,5-h]furo[2,3-b]	43238791	38.439	8.01	1.64	73	303	Complex furoquinoline
7-(Diethylamino)-4-oxofuro[3,2-c]chromene-2-carbaldehyde	2725724	38.975	6.65	0.10	77	285	Furochromone (coumarin derivative)
Lunine	23330991	39.728	11.19	0.88	78	287	Alkaloid
3,5,5-Trimethyl-11-oxo-5,6,6a,11-tetrahydroisoindolo[2,1-a]quinoline	884421	42.030	7.17	0.03	67	321	Alkaloid (isoindoloquinoline)
				100.00			

Molecular interaction analysis demonstrated that Lunacrine established multiple conventional hydrogen bonds and hydrophobic contacts with AMPK, SIRT1, and COX-2. In the AMPK complex, hydrogen bonds and polar interactions were observed with Leu A:22, Ala A:156, Asp A:157, Glu A:94, Gly A:23, Gly A:25, Gly A:99, Ile A:77, Val A:96, and Tyr A:95, along with π-alkyl and hydrophobic contacts involving Val A:30, Leu A:146, and Ala A:43. For SIRT1, Lunacrine interacted with Ala A:262, Ile A:270, Phe A:273, Val A:445, and His A:363, supported by additional non-covalent contacts at Tyr A:280, Asn A:346, and Ile A:347. In the COX-2 complex, key hydrogen bonds and polar interactions were formed with Cys B:36 and Arg B:44, while π-alkyl and van der Waals interactions involved Cys B:47, Leu B:152, Arg B:469, Lys B:468, Pro B:40, and Asn B:39. Meanwhile, fatty acids such as (Z)-11-octadecenoic acid and (9Z,12Z)-octadeca-9,12-dienoic acid formed hydrogen bonds and alkyl interactions with PPAR-α at residues Asp A:353, Gln A:435, Lys A:358, and Phe A:361. Dynein interactions were observed at Leu A:90, Arg A:88, and Pro A:149. These interaction profiles are visually represented in the two-dimensional ligand-protein interaction diagrams shown in Figure 3.A-3.I. These findings support the binding affinity data and provide structural evidence of stable and biologically relevant ligand-target associations.

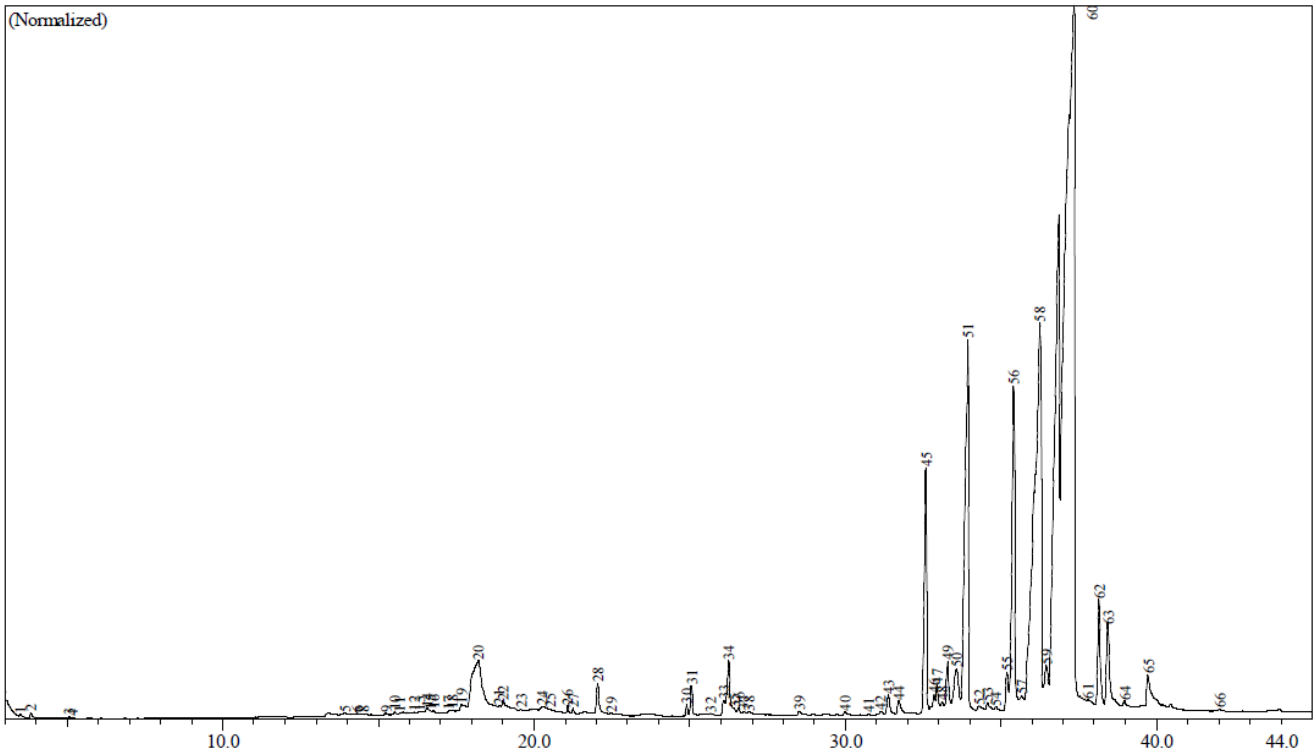

Figure 2. GC-MS chromatogram of KU extract

Table 3. Pharmacokinetic profile of the compounds

Compound	Molecular weight (g/mol)	Hydrogen donor	Hydrogen acceptor	cLogP	TPSA (Å²)	Lipinski criteria	Information
Lunacrine	273.33	0	3	2.80	40.46	Yes	No violation
(Z)-11-Octadecenoic acid	282.46	1	2	5.70	37.30	Yes	1 violation: CLogP>4.15
Hexadecanoic acid	270.45	0	2	5.54	26.30	Yes	1 violation: CLogP>4.15
(9Z,12Z)-Octadeca-9,12-dienoicacid	280.45	1	2	5.88	37.30	Yes	1 violation: CLogP>4.15

Table 4. Results of molecular docking analysis

Compound	Macro-molecule	Binding affinity (kcal/mol)	Recipitor interaction
Lunacrine	AMPK	-7.8	Ala A:156, Ala A:43, Asp A:157, Glu A:94, Gly A:23, Gly A:25, Gly A:99, Ile A:77, Leu A:146, Leu A:22, Met A:93, Tyr A:95, Val A:30, Val A:96
	SIRT1	-8.5	Ala A:262, Arg A:274, Asn A:346, Asp A:272, Asp A:348, Gln A:345, His A:363, Ile A:270, Ile A:347, Phe A:273, Ser A:265, Tyr A:280, Val A:445
	COX-2	-8.9	Arg B:44, Arg B:469, Asn B:39, Asn B:43, Cys B:36, Cys B:41, Cys B:47, Gln B:42, Glu B:46, Glu B:465, Gly B:45, Leu B:152, Lys B:468, Pro B:153, Pro B:40, Tyr B:130
(Z)-11-Octadecenoic acid	PPAR-α	-5.2	Asp A:353, Asp A:360, Asp A:432, Gln A:435, Glu A:439, His A:440, Ile A:354, Leu A:436, Leu A:443, Lys A:358, Lys A:364, Phe A:361, Pro A:357
	Dynein	-3.6	Arg A:88, Asn A:91, Glu A:154, Gly A:150, Leu A:153, Leu A:87, Leu A:90, Lys A:92, Phe A:157, Pro A:149
Hexadecanoic acid	AMPK	-5.1	Arg E:269, Arg E:299, Arg E:70, Glu E:274, His E:298, Ile E:240, Leu E:277, Lys E:170, Phe A:273, Phe E:244, Pro A:367, Ser E:242, Val E:297
	SIRT1	-6.3	Ala A:262, Asn A:346, Asp A:348, Gln A:345, His A:363, Ile A:270, Ile A:347, Ile A:411, Phe A:273, Phe A:297, Phe A:413, Phe A:414, Ser A:265, Val A:412
(9Z,12Z)-Octadeca-9,12-dienoic acid	PPAR-α	-5.0	Asp A:353, Asp A:360, Asp A:432, Gln A:435, Glu A:439, His A:440, Ile A;354, Leu A:436, Leu A:443, Lys A:358, Phe A:361, Pro A:357
	Dynein	-4.6	Arg A:88, Asn A:91, Gly A:150, Leu A:153, Leu A:87, Leu A:90, Lys A:158, Lys A:92, Phe A:157, Pro A:149

To complement the interaction data, three-dimensional visualizations of Lunacrine docked within AMPK, SIRT1, and COX-2 were generated and are presented in Figures 4.A-4.C. These structural models illustrate the spatial orientation and binding conformation of Lunacrine within each protein's active or regulatory site, highlighting hydrogen bonds and hydrophobic contacts that contribute to binding stability. The visualizations provide additional evidence supporting the docking scores and reinforce the relevance of these interactions to potential pharmacological effects.

Discussion

Qualitative phytochemical analysis of KU extract confirmed the presence of flavonoids, alkaloids, tannins, and saponins. Ethanol, as a polar solvent, has been shown to be effective for phytochemical extraction by displacing water in the plant matrix and enhancing the solubility of polar compounds (Bitwell et al. 2023). In contrast, steroids and terpenoids were not detected likely due to their non-polar nature, which reduces their solubility in ethanol. This finding is consistent with the principle of "like dissolves like," which states that polar solvents preferentially dissolve polar compounds and vice versa (Reichardt 2021).

The detection of bioactive secondary metabolites within KU extract indicates several compounds with therapeutic potential for ameliorating reproductive health disorders. Flavonoids, recognized for their antioxidant properties, may provide cellular protection against oxidative damage and contribute to reproductive health by enhancing microvascular circulation and reducing oxidative stress (Adewoyin et al. 2017; Mondal and Rahaman 2020; Bhardwaj et al. 2021). Alkaloids, commonly associated with stimulatory effects, possess the potential to modulate energy homeostasis and sexual function (Brunetti et al. 2020). Tannins, known for their anti-inflammatory properties, may contribute to maintaining reproductive system integrity by mitigating inflammatory processes (Sobhani et al. 2021). Additionally, saponins, known for their immunostimulatory activities, may support reproductive function via immunomodulatory mechanisms (Behl et al. 2021; Cui et al. 2023). However, since this study relied on reagent-based qualitative screening without reference standards, the results should be considered a preliminary identification of phytochemical classes. Quantitative validation using standard-based methods such as TLC, HPLC, or UV-Vis spectroscopy is recommended for future research to enhance analytical rigor and reproducibility.

The interpretation of FTIR spectra provides further evidence for the presence of these phytochemical groups (Figure 1). A broad absorption band around 3398.04 cm^{-1} indicates O-H stretching vibration, typically associated with hydroxyl groups present in alcohols and phenolic compounds, such as flavonoids and tannins (Nandiyanto et al. 2023). The broad nature of this peak suggests the presence of intermolecular hydrogen bonding, a common characteristic of polar plant metabolites (Smith 2022). The C-H stretching vibrations at 2926.15 cm^{-1} and 2855.72 cm^{-1} are attributes to aliphatic chains, indicating the presence of $-CH_2-$ and $-CH_3$ groups typically found in saponins and other hydrocarbon-containing compounds (Pasieczna-Patkowska et al. 2025).

A distinct peak at 1700.21 cm^{-1} indicates C=O stretching, characteristic of carbonyl-containing constituents such as alkaloids or esters (Sokal et al. 2023; Pasieczna-Patkowska et al. 2025). The fingerprint region (below 1500 cm^{-1}), though marked by overlapping and somewhat broad peaks—including bands at 1605.18, 1462.56, 1365.97, and 1034.50 cm^{-1}—indicates the coexistence of various functional groups such as aromatic rings, C-O, and possibly C-N bonds. While the complexity and peak overlaps in this region limit spectra specificity, they reflect the chemically diverse nature of the KU extract, reinforcing the presence of multifunctional bioactive compounds (Özgenç et al. 2017; Nandiyanto et al. 2023).

GC-MS analysis was conducted to identify individual compounds in the KU extract (Figure 2 and Table 2). The identification process involved comparing the mass fragmentation patterns of each detected peak with reference spectra inlibraries. The degree of similarity was quantified using a library matching quality score, also known as the match factor, typically ranging from 0 to 1000.

In this study, only compounds with a match score of ≥850 were considered highly reliable, corresponding to >85% confidence in structural identity, aligning with standard metabolite profiling thresholds (Tsugawa and Fukusaki 2020). Structural annotation was carefully interpreted for peaks with lower match scores (700-849) and further supported by retention time and peak shape analysis.

To minimize false positives, redundant or low-abundance peaks with ambiguous match scores were excluded from docking prioritization. This approach ensured that only structurally well-validated compounds, both in abundance and spectral fidelity, were selected for biological relevance analysis. These GC-MS results strongly support and complement the initial phytochemical screening. While the qualitative phytochemical tests confirmed the presence of flavonoids, alkaloids, tannins, and saponins, several of the dominant compounds identified by GC-MS are known alkaloids, thereby validating the presence of nitrogen-containing bioactive compounds (Bai et al. 2021). Similarly, fatty acids such as (9Z,12Z)-Octadeca-9,12-dienoic acid and (Z)-11-Octadecenoic acid are functionally associated with saponin-related and lipid-soluble phytochemical classes (Collodel et al. 2020; Sena and Denmeade 2021).

The GC-MS analysis of *S. lucida* ethanol extract revealed a chemically diverse and complex profile, with 66 identified compounds. This diversity suggests that *S. lucida* is metabolically active, consistent with reports on other species in the genus. Previous research has shown that Strychnos species possess considerable chemical diversity, particularly in their alkaloid, terpenoid, and phenolic content (Rahayu et al. 2022; Alagbe 2023; Cassas et al. 2025). The ethyl acetate extract of *S. innocua* showed the presence of 37 identified compounds (Ibrahim et al. 2021). The higher number of compounds in this study is likely due to ethanol—a more polar solvent capable of extracting a wide range of constituents, including polar secondary metabolites.

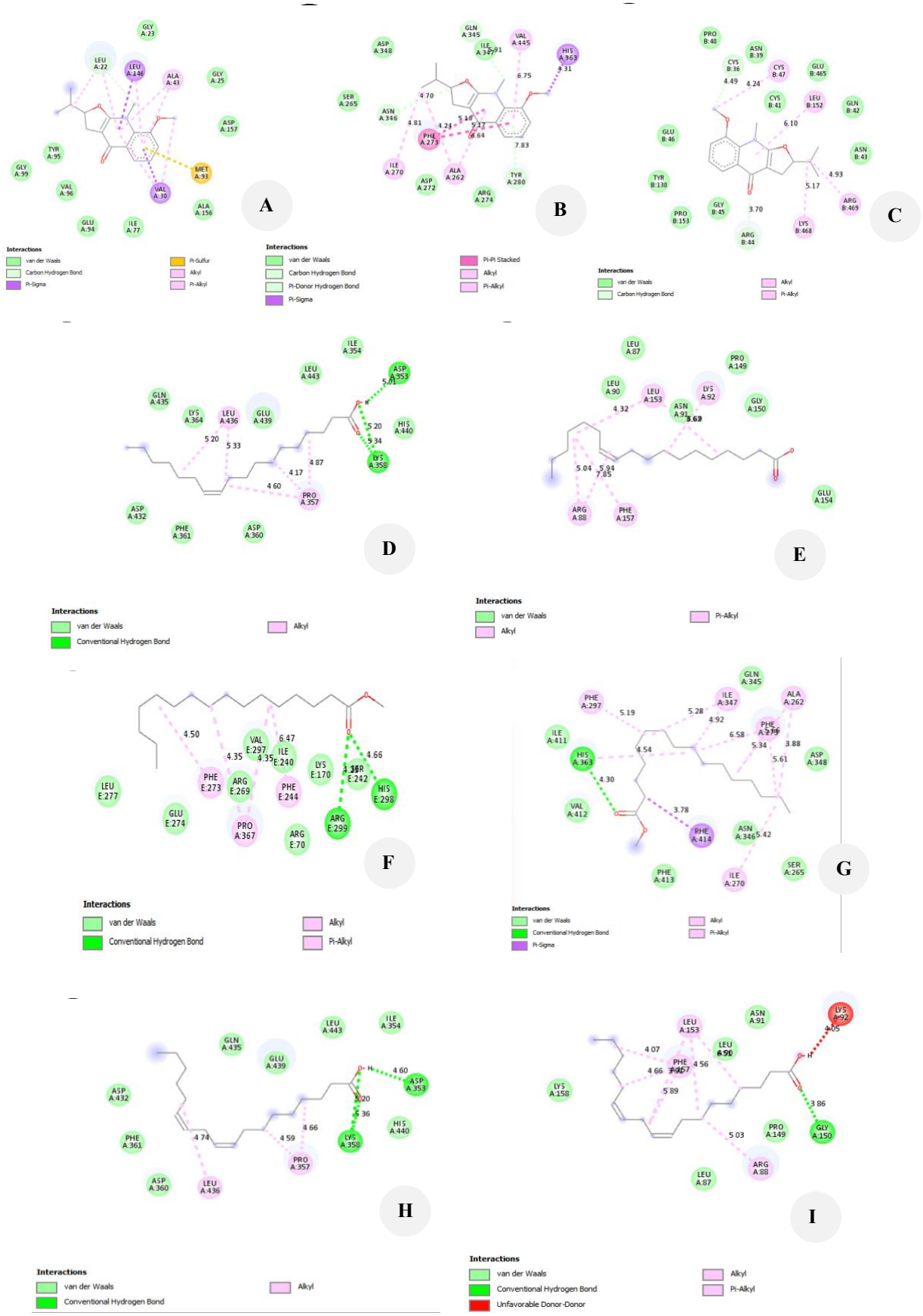

Figure 3. 2D visualization of target receptors and ligands of Kayu Ular extract compounds: A. Lunacrine-AMPK, B. Lunacrine-SIRT1, C. Lunacrine-COX-2, D. (Z)-11-Octadecenoic acid-PPAR-α, E. (Z)-11-Octadecenoic acid-Dynein, F. Hexadecanoic acid-AMPK, G. Hexadecanoic acid-SIRT1, H. (9Z,12Z)-Octadeca-9,12-dienoic acid-PPAR-α, I. (9Z,12Z)-Octadeca-9,12-dienoic acid-Dynein

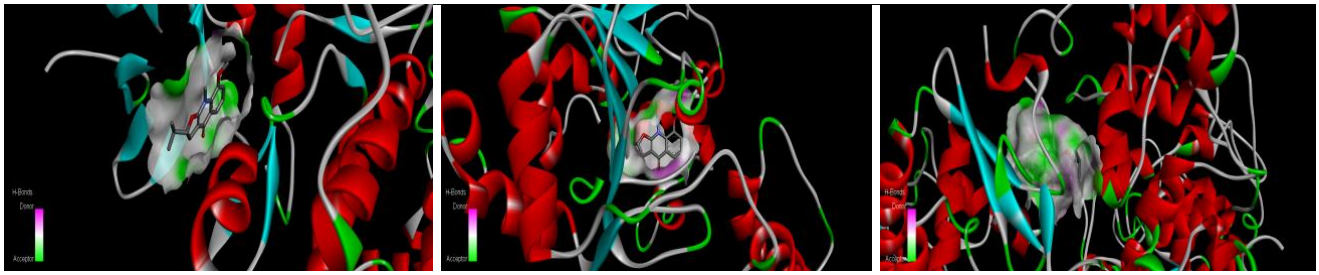

A B C

Figure 4. 3D visualization of Lunacrine within the active sites of: A. AMPK, B. SIRT1, and C. COX-2. Protein structures are displayed in ribbon format (α-helices in red, β-sheets in cyan), and Lunacrine is shown in stick model within the binding pocket. Surface contours represent the receptor cavity, while hydrogen bond donor and acceptor interactions are indicated in magenta and green, respectively. Visualizations were generated using Discovery Studio Visualizer

The extract was dominated by Lunacrine (52.71%) and Balfourodine (15.67%), together accounting for over two-thirds of the total content. Consistent with previous reports indicating that alkaloids are often predominant in *Strychnos* species (Tittikpina et al. 2020; Cassas et al. 2025), this study further highlights the prominence of specific alkaloid constituents. Notably, recent findings in *Strychnos peckii* B.L.Rob. revealed high alkaloid chemodiversity, with 33 alkaloids identified among 46 metabolites (Cassas et al. 2025). This suggests that *S. lucida* may represent a distinct chemotype enriched in specific alkaloids such as Lunacrine. The absence of well-known alkaloids like strychnine and brucine in this study may be attributed to their low abundance, limited solubility in ethanol, or inefficient extraction under the applied conditions.

The ten dominant compounds were selected based on their highest relative abundance in the chromatogram, as they cumulatively accounted for over 80% of the total peak area. This prioritization focused molecular docking simulations on the most chemically representative and biologically relevant constituents (Tsugawa and Fukusaki 2020). However, the 56 minor constituents identified may act synergistically with the major compounds or exert independent bioactivities, thereby contributing to the extract's overall pharmacological profile (Yuan et al. 2016; Behl et al. 2021). Future studies are encouraged to investigate these lower-abundance compounds for their potential additive or modulatory effects. Additionally, the presence of chemical classes such as methyl esters, phenolic acids, and quinoline derivatives indicates a chemical diversity consistent with the initial phytochemical screening of *S. lucida* (Silva et al. 2023).

The pharmacological potential of several identified compounds is particularly noteworthy. Many are known for antimicrobial, antioxidant, and anti-inflammatory properties, which support the ethnomedicinal application of *S. lucida*, particularly in reproductive health. Several compounds, such as β-bisabolene, Neophytadiene, and 2-ethylhexanal, are also associated with their toxicological properties. β-Bisabolene, for example, is associated with dermal irritation and aquatic toxicity (BASF 2023), while Neophytadiene and 2-ethylhexanal have demonstrated oral and respiratory toxicity (MedChemExpress 2023; PubChem 2024). Therefore, toxicity tests are necessary before clinical or veterinary applications, although therapeutic properties are well known. Kunu et al. (2020) reported that *S. lucida* decoction significantly reduced spermatozoa abnormalities in diabetic mice, indicating potential benefits for reproductive health (Kunu et al. 2020). Further investigation is needed to elucidate the mechanisms of action and possible synergistic effects among the extract's constituents.

Molecular docking simulations assessed the potential of KU compounds to modulate reproductive health. However, redocking validation was only performed for COX-2 with limited success, as RMSD values were relatively high (>10 Å). Due to technical limitations, RMSD-based validation was not feasible for other target proteins that do not have corresponding native ligand data. Future studies should incorporate more extensive docking protocol validations, including RMSD analysis, to improve the accuracy of predicted ligand-receptor interactions.

Among the ten most abundant identified compounds in the GC-MS profile, four compounds, i.e., Lunacrine, (Z)-11-octadecenoic acid (cis-vaccenic acid), hexadecanoic acid (palmitic acid), and (9Z,12Z)-octadeca-9,12-dienoic acid (linoleic acid) were selected for molecular docking simulations. This selection was based on their high relative abundance, the presence of functional groups consistent with FTIR spectral data (such as hydroxyl, carbonyl, and aliphatic chains), and alignment with preliminary phytochemical screening results indicating the presence of alkaloids and lipid-related metabolites (Tsugawa and Fukusaki 2020; Nandiyanto et al. 2023).

Lunacrine, the predominant alkaloid, has been shown to exert anti-inflammatory and metabolic-regulatory activities, potentially contributing to enhanced reproductive health by inhibiting inflammatory pathways and promoting mitochondrial biogenesis (Bai et al. 2021; Sultana et al. 2022). Meanwhile, the three fatty acids support reproductive function by modulating hormonal regulation, membrane fluidity, mitochondrial function, and spermatozoa viability (Hu et al. 2018; Kimura et al. 2019; Collodel et al. 2020; Liman et al. 2021; Sena and Denmeade 2021).

In silico pharmacokinetic analysis using SwissADME indicated that all four compounds closely met Lipinski's Rule of Five, which predicts favorable oral bioavailability

and drug-likeness (Table 1) (Daina et al. 2017). These compounds did not violate more than one of the criteria involving hydrogen bond donors and acceptors, molecular weight, octanol-water partition coefficient (log P), and Total Polar Surface Area (TPSA). While these computational predictions provide useful preliminary insights, they do not replace experimental pharmacokinetic data. Therefore, validation in animal models is essential to assess systemic distribution, metabolic stability, and overall safety.

Several other dominant compounds identified in the GC-MS analysis, such as Balfourodine, Isobalfourodine, and Benzo[octahydroacephenanthrylene], were excluded from docking due to lack of unavailable or unvalidated three-dimensional structural data, as well as potential toxicity concerns or lack of relevance to the reproductive targets (MedChemExpress 2023). Similarly, low-abundance or structurally unsuitable compounds, including methyl 4-hydroxy-3-methoxybenzoate and 1,3,4,5-tetrahydroxycyclohexanecarboxylic acid, failed to meet the pharmacokinetic or structural criteria for docking studies.

This multidimensional selection strategy, integrating chemical abundance, structural compatibility, phytochemical evidence, and pharmacokinetic suitability, was applied to prioritize compounds for docking simulations. This approach ensured that the selected compounds were both chemically diverse and biologically plausible. Five proteins were selected as docking targets based on their key roles in reproductive physiology and in molecular pathways: AMPK (PDB ID: 4CFF), SIRT1 (PDB ID: 4ZZI), COX-2 (PDB ID: 6COX), PPAR-α (PDB ID: 3VI8), and Dynein (PDB ID: 8I3J).

AMPK, SIRT1, and COX-2 represent central regulators of cellular metabolism, oxidative stress, and inflammatory responses—mechanisms that are strongly linked to oocyte quality, sperm motility, and hormonal balance (Lai et al. 2019; Yang et al. 2020; Zhao et al. 2020; Alam et al. 2021; D'Angelo et al. 2021; Estienne et al. 2021; Froment et al. 2022; Liu et al. 2024). PPAR-α is involved in lipid metabolism and hormonal signaling, making it relevant to conditions such as PCOS and luteal insufficiency (Santoro et al. 2020; Przybycień et al. 2022; Li et al. 2023). Dynein, a microtubule-associated motor protein, was included for comparison due to its critical structural role in gamete and embryo transport (Canty et al. 2021; Pereira et al. 2023).

The binding affinities of Lunacrine (−8.9 kcal/mol for COX-2, −8.5 for SIRT1, and −7.8 for AMPK) fall within or exceed the range typically observed for natural product ligands with strong receptor affinity (−6.0 to −8.0 kcal/mol) (Ren et al. 2022; Choo and Chai 2023; Muhammed and Aki-Yalcin 2024), as summarized in Table 4. Among (9Z,12Z)-octadeca-9,12-dienoic acid, (Z)-11-octadecenoic acid, and hexadecanoic acid showed moderate binding affinities (−4.6 to −6.3 kcal/mol), consistent with known endogenous ligand interactions with PPAR-α and other lipid-sensitive proteins (Table 4).

Molecular interaction visualizations (Figure 3) using Discovery Studio confirmed that Lunacrine formed multiple hydrogen bonds and hydrophobic contacts with active site residues across AMPK, SIRT1, and COX-2, supporting its high docking scores (Deepasree and Venugopal 2024; Moon 2024; Flores and Jerves 2025). Specifically, Lunacrine interacted with AMPK through hydrogen bonds with Leu A:22, as well as π-alkyl interactions with Val A:30, Leu A:146, and Ala A:43, indicating stable anchoring within the catalytic region—suggesting a role in energy sensing and gamete metabolism (Martin-Hidalgo et al. 2018). For SIRT1, interactions involved Phe273, His363, Arg274, and Asp272 within the active site cleft, implying potential modulation of oxidative stress and deacetylation pathways in reproductive cells (Liu et al. 2018; Zhao et al. 2020). The strongest binding was observed with COX-2, where Lunacrine established conventional hydrogen bonds with Cys36, Arg44, and Gly45, along with hydrophobic and π-alkyl interactions involving Pro40 and Cys47. These residues are located near the allosteric and oxygenase sites—critical regions for prostaglandin biosynthesis, ovulation, and luteal function (Sugimoto et al. 2015). 3D docking visualizations further support these findings, as shown in Figures 4.A-4.C, highlighting the spatial fit and stability of Lunacrine within each protein's binding pocket.

Taken together, the high binding scores and consistent interaction profiles of Lunacrine with AMPK, SIRT1, and COX-2 suggest potential modulation of metabolic and inflammatory pathways essential to reproductive function. Notably, the binding affinity of Lunacrine to COX-2 (−8.9 kcal/mol) is comparable to that of celecoxib (~−9.0 kcal/mol), as reported in validated docking studies using COX-2 inhibitor complexes (Coy-Barrera 2020; Khan et al. 2020). Likewise, its affinity to SIRT1 (−8.5 kcal/mol) is comparable to those of known modulators such as resveratrol (−8.07 kcal/mol) and SRT2104 (−8.0 kcal/mol) (Kim et al. 2018; Chang et al. 2024), indicating that Lunacrine may act as a functional mimic in modulating oxidative stress and mitochondrial signaling.

The pharmacological relevance of Lunacrine is further supported by its methoxylated aromatic scaffold and conjugated heterocycles, which resemble key pharmacophoric features of potent SIRT1/AMPK modulators such as resveratrol, curcumin, and berberine—phytochemicals known to enhance SIRT1 activity and reduce oxidative stress via the SIRT1/AMPK axis (Cho et al. 2022; Wiciński et al. 2023). Notably, recent studies on non-polyphenolic fused-aromatic SIRT1 activators have demonstrated their ability to promote mitochondrial function and antioxidant defense, thereby reinforcing Lunacrine's candidacy as a promising phytotherapeutic agent (Chen and Yeong 2024).

These findings not only place Lunacrine in the same range of binding affinities as well-characterized reference ligands (e.g., celecoxib, resveratrol), but also highlight its unique structural scaffold as a promising alternative pharmacophore. When combined with favorable ADME predictions—indicating good oral bioavailability and systemic exposure—these attributes collectively strengthen its candidacy as a novel modulator of reproductive health. Nevertheless, unlike approved drugs, the pharmacokinetic behavior and safety profile of Lunacrine remain to be validated through experimental in vivo studies.

In addition, unsaturated fatty acids such as [9Z,12Z]-octadeca-9,12-dienoic acid, [Z]-11-octadecenoic acid, and hexadecanoic acid demonstrated moderate binding affinities

(−4.6 to −6.3 kcal/mol) to PPAR-α and AMPK, primarily through hydrogen bonding with residues such as Asp, Lys, and Gln. Although their affinities were moderate, these compounds may support reproductive function through known roles in metabolic and hormonal regulation (Collodel et al. 2020; Sena and Denmeade 2021). This pattern is consistent with structural analyses showing that synthetic PPAR-α agonists, such as pemafibrate, exhibit substantially stronger binding interactions approximately (−7.5 kcal/mol or stronger) via highly specific residue contacts (Yamamoto et al. 2018). Conversely, in silico studies have demonstrated that numerous phytochemicals display moderate but biologically relevant affinities toward PPAR-α/γ, supporting the concept that natural ligands can provide complementary and potentially synergistic modulation of receptor activity (Mandal et al. 2022).

As for Dynein, although some fatty acids exhibited weak docking interactions, Lunacrine was not docked to this target due to the lack of a well-defined small-molecule binding site. Despite Dynein's importance in gamete and embryo transport (Wen et al. 2018; Canty et al. 2021), its classification as a motor protein makes it a less suitable candidate for phytochemical modulation in early-phase docking analyses (He et al. 2023; Pereira et al. 2023).

While Lunacrine demonstrated favorable in silico pharmacokinetic properties, potential safety concerns must still be addressed. Alkaloids structurally similar to Lunacrine have demonstrated hepatotoxic, genotoxic, and cytotoxic effects in vitro (e.g., β-carboline alkaloids causing DNA damage in ovarian and breast cancer cell lines) (Mota et al. 2020; Tecchio et al. 2024; Yu et al. 2025), raising the need for dedicated in vitro toxicity screening on reproductive cell models prior to comprehensive preclinical testing.

This study has several limitations. The pharmacological inferences rely solely on in silico simulations without direct experimental validation, while the qualitative nature of the phytochemical screening, coupled with the absence of RMSD-based docking validation, limits the interpretability of the docking results. To support the translational development of Lunacrine and related compounds, future research should include quantitative phytochemical analyses; experimental binding studies; in vivo pharmacokinetic evaluations to assess systemic distribution and metabolic stability; as well as reproductive toxicology screening using relevant cell models and animal systems (Tan et al. 2022; Guan et al. 2023; Aljohani et al. 2024).

To the best of our knowledge, this is the first comprehensive study integrating GC-MS profiling, phytochemical classification, in silico pharmacokinetic evaluation, and multi-target molecular docking to assess the reproductive health potential of *S. lucida*. The identification of Lunacrine as a dominant acridone alkaloid with strong binding affinities to AMPK, SIRT1, and COX-2, along with the supportive role of unsaturated fatty acids targeting PPAR-α, reveals a promising phytochemical synergy. Together, these findings establish a scientific rationale for advancing *S. lucida* as a phytopharmaceutical candidate for reproductive health.

In conclusion, the ethanol extract of *Strychnos lucida* contains a chemically diverse profile of bioactive compounds, predominantly the alkaloid Lunacrine, alongside several unsaturated fatty acids. Phytochemical screening and spectroscopic analyses confirmed the presence of flavonoids, alkaloids, tannins, and saponins, while GC-MS profiling identified 66 metabolites with potential pharmacological relevance. Molecular docking demonstrated strong binding affinities of Lunacrine to AMPK, SIRT1, and COX-2, indicating its potential role in modulating energy metabolism, oxidative stress, and inflammation—key pathways involved in reproductive regulation. These findings provide scientific support for the traditional use of *S. lucida* and underscore its promise as a phytotherapeutic candidate for reproductive health. Nonetheless, this study presents several limitations, including the absence of experimental validation, restricted geographic sampling, and a lack of assessment regarding compound synergy and metabolic transformation. To address these gaps, future research should incorporate comprehensive in vitro and in vivo studies —particularly reproductive toxicity assays and pharmacokinetic profiling (absorption, distribution, metabolism, and excretion)—alongside mechanistic binding experiments to confirm safety, bioavailability, and molecular relevance. Such investigations will be essential to translate *S. lucida* from an ethnomedicinal resource into a scientifically validated phytopharmaceutical for reproductive health applications.

ACKNOWLEDGEMENTS

Universitas Hasanuddin and Universitas Islam Negeri Alauddin, Makassar, Indonesia, supported this research.

REFERENCES

Adebowale A, Lamb J, Nicholas A, Naidoo Y. 2016. Molecular systematics of southern African monkey orange *Strychnos* L. (Loganiaceae). Kew Bull 71: 17. DOI: 10.1007/s12225-016-9630-0.

Adewoyin M, Ibrahim M, Roszaman R, Md Isa ML, Mat Alewi NA, Abdul Rafa AA, Anuar MNN. 2017. Male infertility: The effect of natural antioxidants and phytocompounds on seminal oxidative stress. Diseases 5 (1): 9. DOI: 10.3390/diseases5010009.

Agamah FE, Mazandu GK, Hassan R, Bope CD, Thomford NE, Ghansah A, Chimusa ER. 2020. Computational/in silico methods in drug target and lead prediction. Brief Bioinform 21 (5): 1663-1675. DOI: 10.1093/bib/bbz103.

Alagbe JO. 2023. Bioactive compounds in ethanolic extract of *Strychnos innocua* root using gas chromatography and mass spectrometry (GC-MS). Drug Discov 17: e4dd1005. DOI: 10.53022/dd/4dd1005.

Alam F, Syed H, Amjad S, Baig M, Khan TA, Rehman R. 2021. Interplay between oxidative stress, SIRT1, reproductive and metabolic functions. Curr Res Physiol 4: 119-124. DOI: 10.1016/j.crphys.2021.03.002.

Aljohani GF, Zakaria NH, Majid FAA, Hudiyanti D, Anuar MNN. 2024. An integrated in silico-in vitro-in vivo approach for pharmacokinetic studies of andrographolide using aqueous extract of *Andrographis paniculata* (Burm. f.) Wall. ex Nees. Indones J Pharm 35 (4): 599-612. DOI: 10.22146/ijp.12745.

Azwanida NN. 2015. A review on the extraction methods use in medicinal plants, principle, strength and limitation. Med Aromat Plants 4 (3): 1000196. DOI: 10.4172/2167-0412.1000196.

Bai R, Yao C, Zhong Z, Ge J, Bai Z, Ye X, Xie T, Xie Y. 2021. Discovery of natural anti-inflammatory alkaloids: Potential leads for the drug discovery for the treatment of inflammation. Eur J Med Chem 213: 113165. DOI: 10.1016/j.ejmech.2021.113165.

BASF. 2023. Beta-bisabolene: safety data sheet. BASF Corporation. https://www.basf.com/global/en.html.

Behl T, Kumar K, Brisc C, Rus M, Nistor-Cseppento DC, Bustea C, Aron RAC, Pantis C, Zengin G, Sehgal A, Kaur R, Kumar A, Arora S, Setia D, Chandel D, Bungau S. 2021. Exploring the multifocal role of phytochemicals as immunomodulators. Biomed Pharmacother 133: 110959. DOI: 10.1016/j.biopha.2020.110959.

Bhardwaj JK, Panchal H, Saraf P. 2021. Ameliorating effects of natural antioxidant compounds on female infertility: A review. Reprod Sci 28 (5): 1227-1256. DOI: 10.1007/s43032-020-00312-5.

Bhati AP, Wan S, Wright DW, Coveney PV. 2017. Rapid, accurate, precise, and reliable relative free energy prediction using ensemble based thermodynamic integration. J Chem Theory Comput 13 (1): 210-222. DOI: 10.1021/acs.jctc.6b00979.

Bitwell C, Indra SS, Luke C, Kakoma MK. 2023. A review of modern and conventional extraction techniques and their applications for extracting phytochemicals from plants. Sci Afr 19: e01585. DOI: 10.1016/j.sciaf.2023.e01585.

Bonnet O, Beniddir MA, Champy P, Kagisha V, Nyirimigabo A, Hamann C, Jgerenaia G, Ledoux A, Tchinda AT, Angenot L, Frédérich M. 2022. Exploration by molecular networking of *Strychnos* alkaloids reveals the unexpected occurrence of strychnine in seven *Strychnos* species. J Toxicon 215: 57-68. DOI: 10.1016/j.toxicon.2022.06.002.

Bougarne N, Weyers B, Desmet SJ, Deckers J, Ray DW, Staels B, De Bosscher K. 2018. Molecular actions of PPARα in lipid metabolism and inflammation. Endocr Rev 39 (5): 760-802. DOI: 10.1210/er.2018-00064.

Brunetti P, Lo Faro AF, Tini A, Busardò FP, Carlier J. 2020. Pharmacology of herbal sexual enhancers: A review of psychiatric and neurological adverse effects. Pharmaceuticals 13: 309. DOI: 10.3390/ph13100309.

Canty JT, Tan R, Kusakci E, Fernandes J, Yildiz A. 2021. Structure and mechanics of dynein motors. Ann Rev Biophys 50: 549-574. DOI: 10.1146/annurev-biophys-111020-101511.

Cassas F, Santos CLG, da Silva FMA, Cass QB. 2025. *Strychnos peckii* B.L. Rob.: Secondary metabolite annotation by liquid chromatography tandem high resolution mass spectrometry with insights from biogenesis. Anal Bioanal Chem 2025: 1-13. DOI: 10.1007/s00216-025-05967-0.

Chang N, Li J, Lin S, Zhang J, Zeng W, Ma G, Wang Y. 2024. Emerging roles of SIRT1 activator, SRT2104, in disease treatment. Sci Rep 14: 5521. DOI: 10.1038/s41598-024-55923-8.

Chang Y, Hawkins BA, Du JJ, Groundwater PW, Hibbs DE, Lai F. 2022. A guide to in silico drug design. Pharmaceutics 15 (1): 49. DOI: 10.3390/pharmaceutics15010049.

Chen P-T, Yeong KY. 2024. New sirtuin modulators: Their uncovering, pharmacophore, and implications in drug discovery. Med Chem Res 33: 1064-1078. DOI: 10.1007/s00044-024-03249-5.

Cho H-M, Zhang M, Park E-J, Lee B-W, Park Y-J, Kim H-W, Pham H-T-T, Chin Y-W, Oh W-K. 2022. Flavonostilbenes isolated from the stems of *Rhamnoneuron balansae* as potential SIRT1 activators. J Nat Prod 85 (1): 70-82. DOI: 10.1021/acs.jnatprod.1c00689.

Choo MZY, Chai CLL. 2023. The polypharmacology of natural products in drug discovery and development. Ann Rep Med Chem 61: 55-100. DOI: 10.1016/bs.armc.2023.10.002.

Collodel G, Castellini C, Lee JC-Y, Signorini C. 2020. Relevance of fatty acids to sperm maturation and quality. Oxid Med Cell Longev 2020: 7038124. DOI: 10.1155/2020/7038124.

Cournia Z, Allen B, Sherman W. 2017. Relative binding free energy calculations in drug discovery: Recent advances and practical considerations. J Chem Inf Model 57 (12): 2911-2937. DOI: 10.1021/acs.jcim.7b00564.

Coy-Barrera E. 2020. Discrimination of naturally-occurring 2-arylbenzofurans as cyclooxygenase-2 inhibitors: Insights into the binding mode and enzymatic inhibitory activity. Biomolecules 10 (2): 176. DOI: 10.3390/biom10020176.

Cui X, Ma X, Li C, Meng H, Han C. 2023. A review: Structure-activity relationship between saponins and cellular immunity. Mol Biol Rep 50 (3): 2779-2793. DOI: 10.1007/s11033-022-08233-z.

Daina A, Michielin O, Zoete V. 2017. SwissADME: A free web tool to evaluate pharmacokinetics, drug-likeness and medicinal chemistry friendliness of small molecules. Sci Rep 7: 42717. DOI: 10.1038/srep42717.

D'Angelo S, Mele E, Di Filippo F, Viggiano A, Meccariello R. 2021. Sirt1 activity in the brain: Simultaneous effects on energy homeostasis and reproduction. Intl J Environ Res Public Health 18 (3): 1243. DOI: 10.3390/ijerph18031243.

Deepasree K, Venugopal S. 2024. Molecular docking and molecular dynamic simulation studies to identify potential terpenes against Internalin A protein of *Listeria monocytogenes*. Front Bioinform 4: 1463750. DOI: 10.3389/fbinf.2024.1463750.

Dubale S, Kebebe D, Zeynudin A, Abdissa N, Suleman S. 2023. Phytochemical screening and antimicrobial activity evaluation of selected medicinal plants in Ethiopia. J Exp Pharmacol 15: 51-62. DOI: 10.2147/jep.s379805.

Engel DMC, Paul M, Chalasani S, Gonsalves L, Ross DA, Chandra-Mouli V, Cole CB, de Carvalho Eriksson C, Hayes B, Philipose A, Beadle S, Ferguson BJ. 2019. A package of sexual and reproductive health and rights interventions—what does it mean for adolescents? J Adolesc Health 65: S41-S50. DOI: 10.1016/j.jadohealth.2019.09.014.

Estienne A, Bongrani A, Ramé C, Kurowska P, Błaszczyk K, Rak A, Ducluzeau P-H, Froment P, Dupont J. 2021. Energy sensors and reproductive Hypothalamo-Pituitary Ovarian axis (HPO) in female mammals: Role of mTOR (mammalian Target of Rapamycin), AMPK (AMP-activated protein Kinase) and SIRT1 (Sirtuin 1). Mol Cell Endocrinol 521: 111113. DOI: 10.1016/j.mce.2020.111113.

Flores D, Jerves C. 2025. Computational comparison of the binding affinity of selective and nonselective NSAIDs to COX 2 using molecular docking. BioNatura J 2: 1-14. DOI: 10.70099/BJ/2025.02.02.3.

Fonmboh DJ, Abah ER, Fokunang TE, Herve B, Teke GN, Rose NM, Borgia NN, Fokunang LB, Andrew BN, Kaba N, Bathelemy N, Ntungwen FC. 2020. An overview of methods of extraction, isolation and characterization of natural medicinal plant products in improved traditional medicine research. Asian J Res Med Pharm Sci 9 (2): 31-57. DOI: 10.9734/ajrimps/2020/v9i230152.

Froment P, Plotton I, Giulivi C et al. 2022. At the crossroads of fertility and metabolism: The importance of AMPK-dependent signaling in female infertility associated with hyperandrogenism. Hum Reprod 37 (6): 1207-1228. DOI: 10.1093/humrep/deac067.

Fumagalli E, Pintor MP, Suhrcke M. 2024. The impact of health on economic growth: A narrative literature review. Health Policy 143: 105039. DOI: 10.1016/j.healthpol.2024.105039.

Guan T, Bian C, Ma Z. 2023. In vitro and in silico perspectives on the activation of antioxidant responsive element by citrus-derived flavonoids. Front Nutr 10: 1257172. DOI: 10.3389/fnut.2023.1257172.

Gunawan E, Toruan AAL, Rusnaeni R, Appa FE. 2022. Aktivitas antikoagulan dari tumbuhan kayu ular (*Strychnos lucida* R. Br.). Jurnal Biologi Papua 14: 129-136. DOI: 10.31957/jbp.1494. [Indonesian]

Gusmailina G, Komarayati S. 2015. Exploration of organic compounds strychnine bush (*Strychnos lucida*) as source of medicines. Pros Sem Nas Masy Biodiv Indon 1: 1741-1746. DOI: 10.13057/psnmbi/m010738.

He S, Gillies JL, Zang JL, Córdoba-Beldad CM, Yamamoto I, Fujiwara Y, Grantham J, DeSantis ME, Shibuya H. 2023. Distinct dynein complexes defined by DYNLRB1 and DYNLRB2 regulate mitotic and male meiotic spindle bipolarity. Nat Commun 14 (1): 1715. DOI: 10.1038/s41467-023-37370-7.

Hidayat S, Zuhud EAM, Widyatmoko D. 2020. Medicinal plants of the Lesser Sunda Islands. IOP Conf Ser: Earth Environ Sci 528: 012017. DOI: 10.1088/1755-1315/528/1/012017.

Hu X, Ge X, Liang W, Shao Y, Jing J, Wang C, Zeng R, Yao B. 2018. Effects of saturated palmitic acid and omega-3 polyunsaturated fatty acids on Sertoli cell apoptosis. Syst Biol Reprod Med 64 (5): 368-380. DOI: 10.1080/19396368.2018.1471554.

Ibrahim H, Uttu AJ, Sallau MS, Iyun ORA. 2021. Gas Chromatography-Mass Spectrometry (GC-MS) analysis of ethyl acetate root bark extract of *Strychnos innocua* (Delile). Beni-Suef Univ J Basic Appl Sci 10: 65. DOI: 10.1186/s43088-021-00156-1.

Inaba K, Mizuno K. 2016. Sperm dysfunction and ciliopathy. Reprod Med Biol 15 (2): 77-94. DOI: 10.1007/s12522-015-0225-5.

Khan A, Diwan A, Thabet HK, Imran M, Bakht MA. 2020. Discovery of novel pyridazine-based cyclooxygenase-2 inhibitors with a promising gastric safety profile. Molecules 25 (9): 2002. DOI: 10.3390/molecules25092002.

Khasanah U, Ariani N, Aprilia YN, Winarsih S. 2022. Phytochemical screening and haem polymerization inhibitory activity of root extract and fractions from *Strychnos lucida* R. Br. Pharmacogn Commun 12 (2): 40-43. DOI: 10.5530/pc.2022.2.10.

Kim MJ, An HJ, Kim DH, Lee B, Lee HJ, Ullah S, Kim SJ, Jeong HO, Moon KM, Lee EK, Yang J, Akter J, Chun P, Moon HR, Chung HY. 2018. Novel SIRT1 activator MHY2233 improves glucose tolerance and reduces hepatic lipid accumulation in db/db mice. Bioorg Med Chem Lett 28 (4): 684-688. DOI: 10.1016/j.bmcl.2018.01.021.

Kimura I, Ichimura A, Ohue-Kitano R, Igarashi M. 2019. Free fatty acid receptors in health and disease. Physiol Rev 100 (1): 171-210. DOI: 10.1152/physrev.00041.2018.

Krakowska-Sieprawska A, Kiełbasa A, Rafińska K, Ligor M, Buszewski B. 2022. Modern methods of pre-treatment of plant material for the extraction of bioactive compounds. Molecules 27 (3): 730. DOI: 10.3390/molecules27030730.

Kulandaisamy A, Lathi V, ViswaPoorani K, Yugandhar K, Gromiha MM. 2017. Important amino acid residues involved in folding and binding of protein-protein complexes. Intl J Biol Macromol 94: 438-444. DOI: 10.1016/j.ijbiomac.2016.10.045.

Kumar P, Rai SK, Sarangi PP. 2024. An in silico study reveals that a C terminal fragment of the adhesion protein Fibulin7 (Fbln7 C) regulates the activation of integrin α5β1 through dynamics of VWA and the hybrid domain in the β1 subunit. J Biomol Struct Dyn 23: 1-20. DOI: 10.1080/07391102.2024.2431189.

Kunu MB, Baszary CDU, Killay A. 2020. Administrated of snake wood (*Strychnos lucida*) to decreased abnormality spermatozoa of mice (*Mus musculus*) diabetes mellitus modeling. Rumphius Pattimura Biol J 2 (2): 37-42. DOI: 10.30598/rumphiusv2i2p037-042.

Lai Z-Z, Yang H-L, Ha S-Y, Chang K-K, Mei J, Zhou W-J, Qiu X-M, Wang X-Q, Zhu R, Li D-J, Li M-Q. 2019. Cyclooxygenase-2 in endometriosis. Intl J Biol Sci 15: 2783-2792. DOI: 10.7150/ijbs.35128.

Latolla N, Reddy S, van de Venter M, Hlangothi B. 2024. Phytochemical composition, cytotoxicity, antioxidant, and antidiabetic enzyme inhibition potential of *Strychnos henningsii* Gilg. S Afr J Bot 174: 894-901. DOI: 10.1016/j.sajb.2024.09.054.

Laumonier Y, Nasi R. 2018. The last natural seasonal forests of Indonesia: Implications for forest management and conservation. Appl Veg Sci 21 (3): 461-476. DOI: 10.1111/avsc.12377.

Li S, Liu X, Chen X, Bi L. 2020. Research progress on anti-inflammatory effects and mechanisms of alkaloids from Chinese medical herbs. Evid Based Complement Alternat Med 2020: 1303524. DOI: 10.1155/2020/1303524.

Li Y, Zhan M, Li J, Zhang W, Shang X. 2023. Lycopene alleviates lipopolysaccharide-induced testicular injury in rats by activating the PPAR signaling pathway to integrate lipid metabolism and the inflammatory response. Transl Androl Urol 12 (2): 271-285. DOI: 10.21037/tau-22-864.

Liman MS, Franco V, Cardoso CL, Longobardi V, Gasparrini B, Wheeler MB, Rubessa M, Esposito G. 2021. Effects of dietary supplementation of conjugated linoleic acids and their inclusion in semen extenders on bovine sperm quality. Animals 11: 483. DOI: 10.3390/ani11020483.

Liu M, Guo S, Li X, Tian Y, Yu Y, Tang L, Sun Q, Zhang T, Fan M, Zhang L, Xu Y, An J, Gao X, Han L, Zhang L. 2024. Semaglutide alleviates ovary inflammation via the AMPK/SIRT1/NF-κB signaling pathway in polycystic ovary syndrome mice. Drug Des Devel Ther 18: 3925-3938. DOI: 10.2147/dddt.s484531.

Liu Y, Colby JK, Zuo X, Jaoude J, Wei D, Shureiqi I. 2018. The role of PPAR-δ in metabolism, inflammation, and cancer: many characters of a critical transcription factor. Intl J Mol Sci 19 (11): 3339. DOI: 10.3390/ijms19113339.

Makani I, Marenga W, Lekgoba T, Rantong G, Sithole NT, Ntuli F, Kandjou V, Renu R. 2025. The characteristics and efficiency of *Strychnos potatorum* as a medicinal plant and water purification agent: A review. Intl J Environ Sci Technol 22: 9781-9792. DOI: 10.1007/s13762-025-06398-1.

Mandal SK, Kumar BK, Sharma PK, Murugesan S, Deepa PR. 2022. In silico and in vitro analysis of PPAR-α/γ dual agonists: Comparative evaluation of potential phytochemicals with anti-obesity drug orlistat. Comput Biol Med 147: 105796. DOI: 10.1016/j.compbiomed.2022.105796.

Manurung H, Sari RK, Syafii W, Cahyaningsih U, Ekasari W. 2019. Antimalarial activity and phytochemical profile of ethanolic and aqueous extracts of bidara laut (*Strychnos ligustrina* Blum) wood. J Korean Wood Sci Technol 47 (5): 587-596. DOI: 10.5658/wood.2019.47.5.587.

Martin-Hidalgo D, Hurtado de Llera A, Calle-Guisado V, Gonzalez-Fernandez L, Garcia-Marin L, Bragado MJ. 2018. AMPK function in mammalian spermatozoa. Intl J Mol Sci 19 (11): 3293. DOI: 10.3390/ijms19113293.

MedChemExpress. 2023. Neophytadiene: Safety and pharmacological profile. https://www.medchemexpress.com/Neophytadiene.html

Mondal S, Rahaman ST. 2020. Flavonoids: A vital resource in healthcare and medicine. Pharm Pharmacol Intl J 8 (2): 91-104. DOI: 10.15406/ppij.2020.08.00294.

Moon DO. 2024. Plant-derived flavonoids as AMPK activators: Unveiling their potential in type 2 diabetes management through mechanistic insights, docking studies, and pharmacokinetics. Appl Sci 14 (19): 8607. DOI: 10.3390/app14198607.

Mota NSRS, Kviecinski MR, Felipe KB, Grinevicius VMAS, Siminski T, Almeida GM, Zeferino RC, Pich CT, Filho DW, Pedrosa RC. 2020. β-carboline alkaloid harmine induces DNA damage and triggers apoptosis by a mitochondrial pathway: Study in silico, in vitro and in vivo. Intl J Funct Nutr 1 (1): 1. DOI: 10.36105/ijfn.2020v01.01.001.

Muhammed MT, Aki-Yalcin E. 2024. Molecular docking: Principles, advances, and its applications in drug discovery. Lett Drug Des Discov 21: 480-495. DOI: 10.2174/1570180819666220922103109.

Nandiyanto ABD, Ragadhita R, Fiandini M. 2023. Interpretation of Fourier Transform Infrared Spectra (FTIR): A practical approach in the polymer/plastic thermal decomposition. Indones J Sci Technol 8 (1): 113-126. DOI: 10.17509/ijost.v8i1.53297.

Özgenç Ö, Durmaz S, Boyaci IH, Eksi-Kocak H. 2017. Determination of chemical changes in heat-treated wood using ATR-FTIR and FT Raman spectrometry. Spectrochim Acta A Mol Biomol Spectrosc 171: 395-400. DOI: 10.1016/j.saa.2016.08.026.

Pagadala NS, Syed K, Tuszynski J. 2017. Software for molecular docking: A review. Biophys Rev 9: 91-102. DOI: 10.1007/s12551-016-0247-1.

Pasieczna-Patkowska S, Cichy M, Flieger J. 2025. Application of Fourier Transform Infrared (FTIR) spectroscopy in characterization of green synthesized nanoparticles. Molecules 30 (3): 684. DOI: 10.3390/molecules30030684.

Patalas-Krawczyk P, Malinska D, Walczak J, Kratzer G, Prill M, Michalska B, Drabik K, Titz B, Eb-Levadoux Y, Schneider T, Szymanski J, Hoeng J, Peitsch MC, Duszynski J, Szczepanowska J, der Toorn MV, Mathis C, Wieckowski MR. 2021. Effects of plant alkaloids on mitochondrial bioenergetic parameters. Food Chem Toxicol 154: 112316. DOI: 10.1016/j.fct.2021.112316.

Pereira R, Carvalho V, Dias C, Barbosa T, Oliveira J, Alves Â, Oliveira E, Sá R, Sousa M. 2023. Characterization of a DRC1 null variant associated with primary ciliary dyskinesia and female infertility. J Assist Reprod Genet 40 (4): 765-778. DOI: 10.1007/s10815-023-02755-6.

Przybycień P, Gąsior-Perczak D, Placha W. 2022. Cannabinoids and PPAR ligands: The future in treatment of polycystic ovary syndrome women with obesity and reduced fertility. Cells 11 (16): 2569. DOI: 10.3390/cells11162569.

PubChem. 2024. 2-ethylhexanal - compound summary. National Center for Biotechnology Information.

Rahayu AAD, Prihantini AI, Krisnawati, Nugraheni YMMA. 2022. Chemical components of different parts of Strychnos ligustrina, a medicinal plant from Indonesia. IOP Conf Ser: Earth Environ Sci 959: 012061. DOI: 10.1088/1755-1315/959/1/012061.

Reichardt C. 2021. Solvation effects in organic chemistry: A short historical overview. J Org Chem 87: 1616-1629. DOI: 10.1021/acs.joc.1c01979.

Ren M, Wang Y, Lin L, Li S, Ma Q. 2022. α-linolenic acid screened by molecular docking attenuates inflammation by regulating Th1/Th2 imbalance in ovalbumin-induced mice of allergic rhinitis. Molecules 27 (18): 5893. DOI: 10.3390/molecules27185893.

Santoro M, De Amicis F, Aquila S, Bonofiglio D. 2020. Peroxisome proliferator-activated receptor gamma expression along the male genital system and its role in male fertility. Hum Reprod 35 (9): 2072-2085. DOI: 10.1093/humrep/deaa153.

Sembiring MH, Nursanti O, Rahmania TA. 2023. Molecular docking and toxicity studies of nerve agents against Acetylcholinesterase (AChE). J Recept Signal Transduct Res 43 (5): 115-122. DOI: 10.1080/10799893.2023.2298899.

Sena LA, Denmeade SR. 2021. Fatty acid synthesis in prostate cancer: Vulnerability or epiphenomenon? Cancer Res 81 (17): 4385-4393. DOI: 10.1158/0008-5472.can-21-1392.

Setubal RB, Struwe L, Forzza RC. 2025. Revision of *Strychnos* sect. *Breviflorae* subsect. *Eriospermae* (Loganiaceae): A fibrous testa seeded group. Brittonia 77: 85-121. DOI: 10.1007/s12228-024-09822-x.

Setyayudi A, Krisnawati K, Nandini R. 2019. Exploration of bidara laut (*Strychnos lucida*) parent trees in Gunung Tunak Ecotourism Park, West Nusa Tenggara, Indonesia. Biodiversitas 20 (1): 274-278. DOI: 10.13057/biodiv/d200144.

Silva MC, Cunha G, Firmino P, Sallum LO, Menezes A, Dutra J, de Araujo-Neto J, Batista AA, Ellena J, Napolitano HB. 2023. Structural and anticancer studies of methoxyflavone derivative from *Strychnos pseudoquina* A. St.-Hil. (Loganiaceae) from Brazilian Cerrado. ACS Omega 8 (43): 40764-40774. DOI: 10.1021/acsomega.3c05841.

Singh DB, Pathak RK. 2020. Computational approaches in drug designing and their applications. In: Gupta N, Gupta V (eds). Experimental Protocols in Biotechnology. Springer Protocols Handbooks, Humana, New York, NY. DOI: 10.1007/978-1-0716-0607-0_6.

Sladden T, Philpott A, Braeken D, Castellanos-Usigli A, Yadav V, Christie E, Gonsalves L, Mofokeng T. 2021. Sexual health and wellbeing through the life course: Ensuring sexual health, rights and pleasure for all. Intl J Sex Health 33: 565-571. DOI: 10.1080/19317611.2021.1991071.

Smith BC. 2022. The infrared spectra of polymers, VI: Polymers with C-O bonds. Spectroscopy 37: 15-19. DOI: 10.56530/spectroscopy.ly3071f5.

Sobhani M, Farzaei MH, Kiani S, Khodarahmi R. 2021. Immunomodulatory; anti-inflammatory/antioxidant effects of polyphenols: A comparative review on the parental compounds and their metabolites. Food Rev Intl 37 (8): 759-811. DOI: 10.1080/87559129.2020.1717523.

Sokal A, Wrzalik R, Klimontko J, Chrobak E, Bębenek E, Kadela-Tomanek M. 2023. 5,8-Quinolinedione attached to quinone derivatives: XRD diffraction, fourier transform infrared spectra and computational analysis. Molbank 2023 (4): M1747. DOI: 10.3390/M1747.

Souza TAA, Menezes ACS, Santos CKG, Jesus FG, Rocha EC, Araújo MS. 2024. Toxicity of bioactive compounds of *Strychnos pseudoquina* (Loganiaceae) in *Spodoptera frugiperda* (Noctuidae). Sustainability 16 (11): 4430. DOI: 10.3390/su16114430.

Starrs AM, Ezeh AC, Barker G et al. 2018. Accelerate progress—sexual and reproductive health and rights for all: Report of the Guttmacher-Lancet Commission. Lancet 391 (10140): 2642-2692. DOI: 10.1016/S0140-6736(18)30293-9.

Sugimoto Y, Inazumi T, Tsuchiya S. 2015. Roles of prostaglandin receptors in female reproduction. J Biochem 157 (2): 73-80. DOI: 10.1093/jb/mvu081.

Sultana A, Rahman K, Heyat MBB, Sumbul, Akhtar F, Muaad AY. 2022. Role of inflammation, oxidative stress, and mitochondrial changes in premenstrual psychosomatic behavioral symptoms with anti-inflammatory, antioxidant herbs, and nutritional supplements. Oxid Med Cell Longev 2022: 3599246. DOI: 10.1155/2022/3599246.

Surpeta B, Sequeiros-Borja CE, Brezovsky J. 2020. Dynamics, a powerful component of current and future in silico approaches for protein design and engineering. Intl J Mol Sci 21 (8): 2713. DOI: 10.3390/ijms21082713.

Tan H, Wu J, Zhang R, Zhang C, Li W, Chen Q, Zhang X, Yu H, Shi W. 2022. Development, validation, and application of a human reproductive toxicity prediction model based on adverse outcome pathway. Environ Sci Technol 56: 12391-12403. DOI: 10.1021/acs.est.2c02242.

Tecchio KB, de Moura Alves F, Alves JD, de Souza Barbosa C, Salgado MAR, da Silva Vieira Dos Santos VJ, de Pilla Varotti F, de Almeida Campos-Junior PH, Viana GHR, Dos Santos FV. 2024. Evaluation of the in vivo acute toxicity and in vitro genotoxicity and mutagenicity of synthetic β-carboline alkaloids with selective cytotoxic activity against ovarian and breast cancer cell lines. Mutat Res Genet Toxicol Environ Mutagen 899: 503808. DOI: 10.1016/j.mrgentox.2024.503808.

Tittikpina NK, Atakpama W, Hoekou Y, Diop YM, Batawila K, Akapagana K. 2020. *Strychnos spinosa* Lam: Comprehensive review on its medicinal and nutritional uses. Afr J Tradit Complement Altern Med 17 (2): 8-28. DOI: 10.21010/ajtcam.v17i2.2.

Travasarou A, Angelopoulou MT, Vougogiannopoulou K, Papadopoulou A, Aligiannis N, Cantrell CL, Kletsas D, Fokialakis N, Pratsinis H. 2019. Bioactive metabolites of the stem bark of *Strychnos* aff. *darienensis* and evaluation of their antioxidant and UV protection activity in human skin cell cultures. Cosmetics 6 (1): 7. DOI: 10.3390/cosmetics6010007.

Tsugawa H, Fukusaki E. 2020. Effectiveness of metabolomics research using gas chromatograph/quadrupole mass spectrometer with high-sensitivity and high-speed scanning. Shimadzu Tech Rep C146-C217: 1-6.

Tuli H, Sood S, Pundir A, Choudhary D, Dhama K, Kaur G, Seth P, Vashishth A, Kumar P. 2022. Molecular docking studies of apigenin, kaempferol, and quercetin as potential targets against spike receptor protein of SARS-CoV. J Exp Biol Agric Sci 10 (1): 144-149. DOI: 10.18006/2022.10(1).144.149.

Ukwubile CA, Malgwi TS, Menkiti ND. 2024. Examining the isolation of bioactive compounds, antinociceptive, and anti-inflammatory activities of *Strychnos spinosa* Lam. (Loganiaceae) stembark extract. Pharm Biomed Res 10 (1): 23-32. DOI: 10.32598/PBR.10.1.1162.1.

Wan S, Bhati AP, Zasada SJ, Coveney PV. 2020. Rapid, accurate, precise and reproducible ligand-protein binding free energy prediction. Interface Focus 10 (6): 20200007. DOI: 10.1098/rsfs.2020.0007.

Wen Q, Tang EI, Lui W-Y, Lee WM, Wong CKC, Silvestrini B, Cheng CY. 2018. Dynein 1 supports spermatid transport and spermiation during spermatogenesis in the rat testis. Am J Physiol Endocrinol Metab 315 (5): E924-E948. DOI: 10.1152/ajpendo.00114.2018.

WHO [World Health Organization]. 2018. WHO recommendations on adolescent sexual and reproductive health and rights. WHO, Geneva.

Wiciński M, Erdmann J, Nowacka A, Kuźmiński O, Michalak K, Janowski K, Ohla J, Biernaciak A, Szambelan M, Zabrzyński J. 2023. Natural phytochemicals as SIRT activators-Focus on potential biochemical mechanisms. Nutrients 15 (16): 3578. DOI: 10.3390/nu15163578.

Yamamoto Y, Takei K, Arulmozhiraja S, Sladek V, Matsuo N, Han S-I, Matsuzaka T, Sekiya M, Tokiwa T, Shoji M, Shigeta Y, Nakagawa Y, Tokiwa H, Shimano H. 2018. Molecular association model of PPARα and its new specific and efficient ligand, pemafibrate: Structural basis for SPPARMα. Biochem Biophys Res Commun 499 (2): 239-245. DOI: 10.1016/j.bbrc.2018.03.135.

Yang W, Wang L, Wang F, Yuan S. 2020. Roles of AMP-activated protein Kinase (AMPK) in mammalian reproduction. Front Cell Dev Biol 8: 593005. DOI: 10.3389/fcell.2020.593005.

Younus S, Vinod Chandra SS, Nair ASS. 2021. Docking and dynamic simulation study of crizotinib and temozolomide drug with glioblastoma and NSCLC target to identify better efficacy of the drug. Future J Pharm Sci 7: 187. DOI: 10.1186/s43094-021-00323-2.

Yu L, Shen N, Ren J, Xin H, Cui Y. 2025. Resource distribution, pharmacological activity, toxicology and clinical drugs of β-carboline alkaloids: an updated and systematic review. Fitoterapia 180: 106326. DOI: 10.1016/j.fitote.2024.106326.

Yuan H, Ma Q, Ye L, Piao G. 2016. The traditional medicine and modern medicine from natural products. Molecules 21 (5): 559. DOI: 10.3390/molecules21050559.

Yueniwati Y, Syaban MFR, Faratisha IFD, Yunita KC, Kurniawan DB, Putra GFA, Erwan NE. 2021. Molecular docking approach of natural compound from herbal medicine in Java against severe acute respiratory syndrome coronavirus-2 receptor. Maced J Med Sci 9: 1181-1186. DOI: 10.3889/oamjms.2021.6963.

Zhao L, Cao J, Hu K, He X, Yun D, Tong T, Han L. 2020. Sirtuins and their biological relevance in aging and age-related diseases. Aging Dis 11 (4): 927-945. DOI: 10.14336/AD.2019.0820.